ГЛАСНИК Српског географског друштва 105(1) 67-82
BULLETIN OF THE SERBIAN GEOGRAPHICAL SOCIETY 2025

Original scientific paper UDC 556.55(594)
https://doi.org/10.2298/GSGD2501067J

Received: October 25, 2024
Corrected: November 26, 2024
Accepted: November 27, 2024

Atriyon Julzarika[1*], Argo Galih Suhadha[*]

* *The National Research and Innovation Agency (BRIN), Indonesia*

DYNAMICS OF CHANGES IN LAKE VOLUME AND SURFACE AREA USING MULTI-SOURCE GEOSPATIAL DATA

Abstract: Geospatial technology has advanced significantly, with modern sensors installed on satellites, terrestrial geodetic survey tools, and aerial devices. These developments allow for the integration of old topographic maps, satellite geospatial data, and bathymetric measurements to study the dynamics of lake volume and surface area. Testing was conducted on Lake Singkarak, a tectonic lake in West Sumatra, Indonesia. The main objective of this study is to monitor the dynamics of changes in the volume and surface area of Lake Singkarak from 1883 to 2023 using multi-source geospatial data. The Dutch East Indies topography-bathymetry (1883) map and the DTM/bathymetry (2023) data were used. All of the data were aligned to a similar map system, namely the horizontal datum (WGS 1984), the vertical datum (EGM 2008), and the projection system (UTM). The DTM/bathymetry (1883) model was extracted based on digitization, and then 3D visualization was performed. The DTM/bathymetry (2023) model was extracted by integrating the latest DTM and field measurements. The latest DTM was obtained from the DTM/bathymetry (2017) (integration of field measurement with satellite imagery 2017), which was then updated with the time-series vertical deformation (2017-2022). After that, the latest DTM was integrated with the field measurement (2023) data to obtain the DTM/bathymetry (2023). A comparison of the 1883 and 2023 models reveals an increase in volume by 2.64 billion m^3, a change in the addition of perimeter of 4,509 km, and a change in the decrease in surface area of 1.14 km^2. The major earthquake and tsunami in Lake Singkarak in 1926 most likely caused these changes. The results of this modeling can be used for policies in regional planning and disaster mitigation in Lake Singkarak.

Keywords: lake Singkarak, volume and surface area, dynamics changing, topography maps, DTM/bathymetry

[1] verbhakov@yahoo.com (corresponding author)
Atriyon Julzarika (https://orcid.org/0000-0002-4531-5327)
Argo Galih Suhadha (https://orcid.org/0000-0001-5970-9194)

Introduction

Geospatial technology has undergone significant advancements in recent years, revolutionizing how we conduct mapping surveys with high-accuracy and precision sensors (Julzarika et al., 2023; Koman et al., 2023). The development of high-accuracy and precision sensors has caused the cost and time of mapping surveys to become faster (Vazirabad & Karslioglu, 2010; Maune & Nayegandhi, 2018). These sensors are installed on satellites, aircraft, unmanned aerial vehicles (UAVs), and terrestrial survey tools (Julzarika & Djurdjani, 2018; Liu et al., 2018; NASA, 2018).

The technology's advancement is marked by changes in land topographic mapping surveys and underwater topographic mapping surveys (bathymetry) (Siermann et al., 2014; Maune & Nayegandhi, 2018). Historically, bathymetric mapping relied on direct measurement tools such as the lead line method. 3D modeling is done by on-screen digitization and displayed as 3D contours. The visualization can be seen as a series of lines that describe certain elevation values (Li et al., 2004). Unlike the current conditions, bathymetry extraction can be done with sonar, LiDAR, and satellite imagery (Champion & Boldo, 2006; Krauß et al., 2011; Siermann et al., 2014).

Today, advanced bathymetric methods include Interferometry Synthetic Aperture Sonar (IFSAS), Singlebeam Echosounder (SBES), Multibeam Echosounder (MBES), and Light Detection and Ranging (LiDAR) bathymetry. Additionally, satellite-derived bathymetry (SDB), liqui interferometry synthetic aperture radar (Liqui-InSAR), and digital elevation model (DEM) integration from various sensors have become essential in modern mapping (Tarikhi, 2012; Wensink & Alpers, 2015; Julzarika & Djurdjani, 2018; Maune & Nayegandhi, 2018; Koman et al., 2023). Although there are differences in accuracy and precision, bathymetric data can determine how the lake bed has changed to current conditions. These changes are useful in understanding the dynamics of the lake bed, volume, surface area, and topographic footprint (Finkl et al., 2005; Maune & Nayegandhi, 2018; Shen, 2018).

The development of geospatial technology is marked by old topographic maps that still use simple measuring instruments. However, sophisticated sensors have been developed that are installed on satellites, terrestrial geodetic survey tools, and aerial (Maune & Nayegandhi, 2018). Data sources of old topographic maps, satellite geospatial data, and bathymetric measurements can be used to determine the dynamics of the volume and surface area of the lake.

One example of a region where historical geospatial data has been valuable is Lake Singkarak. The Dutch East Indies survey department created a topographic map of the lake, offering a rich source of historical geospatial data for modern comparisons (Julzarika et al., 2021a; Purnama et al., 2023). The old Dutch East Indies topographic map is one example of multi-source geospatial data. On the map, there is land contour and depth contour information related to geospatial information on Lake Singkarak and its surroundings.

Multi-source geospatial data, including old maps, satellite imagery, aerial photography, sonar measurements, and vertical deformation data, provides a comprehensive basis for analyzing regional dynamics such as Lake Singkarak's (ASPRS, 2014; Maune & Nayegandhi, 2018; Julzarika et al., 2022; Koman et al., 2023). Various geospatial data sources can be used to analyze the region's dynamics and track records, such as Lake Singkarak earlier. One of the requirements that must be met in the use of multiple sources of geospatial data is the alignment of the map system of all data used (Wang et al., 2015; Julzarika et al., 2023). The alignment of the map system is in the form of a map projection system, coordinate system, horizontal datum, and vertical datum.

Geospatial technology can map Lake Singkarak's dynamics (Julzarika & Harintaka, 2019; Julzarika et al., 2021a). One way is to monitor volume and surface area changes from the old topography map 1883 to the digital terrain model (DTM)/bathymetry 2023 data. This monitoring also involves vertical deformation parameters to know which areas in Lake Singkarak have the potential for tectonic uplift and subsidence and which areas have experienced extreme landslides from 1883 to 2023. The old topography map of 1883 was created by the Dutch East Indies survey mapping agency with information on land height points and depth points in Lake Singkarak. Meanwhile, the DTM/bathymetry 2023 is the latest DTM extracted from the integration of WorldView-3, Sentinel-1 satellite imagery, field data measurements, DTM 2017, and vertical deformation 2017-2023 (Julzarika et al., 2020; Julzarika, 2021; Julzarika et al., 2021a). This study highlights the transformative role of multi-source geospatial data in understanding the dynamic changes in lake volume and surface area over time, providing insights that are crucial for environmental monitoring and land management. The main objective of this study is to monitor the dynamics of changes in the volume and surface area of Lake Singkarak from 1883 to 2023 using multi-source geospatial data.

Materials and methods

Study area

The study focuses on Lake Singkarak in West Sumatra, Indonesia (see Figure 1). As the second-largest lake on Sumatra Island, Lake Singkarak is a tectonic lake situated at an elevation of 364 m (Geological, 2017; Julzarika et al., 2021a; Purnama et al., 2023). It is intersected by the Semangko Fault, a significant geological feature that runs north to south across the island (Verstappen, 1961).

Lake Singkarak is one of the national lake priority areas in Indonesia. The border area of Lake Singkarak (2/3 area) is located in Tanah Datar Regency and Solok Regency (1/3 area). These administrative divisions result in differing management practices, particularly concerning the maintenance of the lake's aquatic environment. Tanah Datar Regency benefits from indigenous local wisdom, leading to more effective environmental protection of Lake Singkarak compared to Solok Regency. The lake has two main outlets in Tanah Datar Regency: the Umbilin River and the Singkarak Hydroelectric Power Plant (Finaldhi, 2018). In contrast, the lake receives inflow from several rivers, predominantly originating in Solok Regency (Purnama et al., 2023). In Tanah Datar Regency, the areas surrounding Lake Singkarak are characterized by forests, steppes, and settlements. Conversely, Solok Regency's portion of the lake is predominantly bordered by agricultural lands and settlements (Ajiwibowo et al., 2019; Wils et al., 2021).

Lake Singkarak is crossed by the Semangko Fault, causing the eastern side of the lake to become a semi-arid area dominated by steppes and rugged rocks and has low rainfall (Julzarika & Harintaka, 2019). The western area of the lake is a tropical forest with very high rainfall, making it prone to landslides. The center of the Semangko fault is located north of Lake Singkarak, precisely on Gunung Rajo, Batipuh, Tanah Datar Regency (Geological, 2017; Julzarika & Harintaka, 2019; Julzarika et al., 2021a; Falah et al., 2023). On the northern side of the lake, remnants of ancient structures have been discovered, possibly submerged due to a major earthquake or the eruption of Mount Sitinjau—currently known as Lake Maninjau (Verstappen, 1961). The Semangko fault crack in Lake Singkarak is getting wider and deeper (Julzarika & Harintaka, 2019). Between 2017 and 2019, vertical deformation measurements revealed tectonic subsidence ranging from -10 to -15 cm and an average uplift of 15.79 cm (Julzarika & Harintaka, 2019). Lake Singkarak is surrounded by volcanic rocks and bedrock from the West Sumatra block, which is exposed in the western part of the lake. Lake Singkarak is oriented along the Semangko Fault, formed by dextral shifting in the overlapping Sumani and Sianok segments.

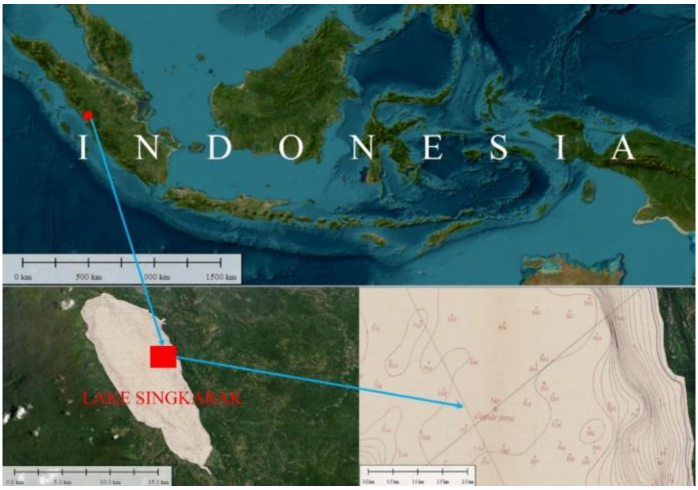

Fig. 1. Map of the study area: Lake Singkarak, West Sumatra, Indonesia. The background imagery of Indonesia is sourced from World Imagery 2023, while Lake Singkarak imagery is derived from WorldView-3 and an old topography (bathymetry) map of the Dutch East Indies.

Previous studies on Lake Singkarak have focused on various aspects, including water quality assessment, water catchment areas, Bilih fish potential, water fertility levels, environmental quality monitoring, land cover, erosion rates, and the seismicity of the Semangko Fault (Mukti, 2018; Falah et al., 2023). Lake Singkarak is a product of tectonic processes influenced by the Sumatra Fault and is part of the Singkarak-Solok Basin segment (Wils et al., 2021; Falah et al., 2023). The basin of this lake was formed from subsidence caused by the movement activity of the Sumatra Fault (Verstappen, 1961). This large basin is dammed by volcanic material from the surrounding volcanic eruptions. As a result of the damming of this volcanic material, Lake Singkarak was formed in one part of the Singkarak-Solok Basin. Lake Singkarak was formed mainly by tectonic processes (Finaldhi, 2018).

The frequent occurrence of large earthquake activity in the Semangko Fault causes the lake bed to be crossed by two parts of the Semangko Fault and become very dynamic (Julzarika & Harintaka, 2019; Wils et al., 2021). The steep underwater topography causes the potential for post-earthquake landslides to be high. The events before the earthquake were marked by long-term subsidence, but when the earthquake occurred, uplift occurred. The instability of the rocks and steep slopes will cause landslides after the uplift. Notably, a significant tsunami occurred in Lake Singkarak following the Padang Panjang earthquake in 1926 (Verstappen, 1961; Geological, 2017; Wils et al., 2021).

Methodology

Data

The data used in this study are an old topographic map of the Dutch East Indies in 1883 from the Leiden University web, bathymetry 2023, field measurement (depth point sonar 2017 and 2023) data, DTM 2017, vertical deformation 2017-2023, height measurements with global navigational satellite system (GNSS) leveling in 2017 and 2023 for land topography around the lake, World Imagery from Global Mapper cloud, and WorldView-3 imagery in 2023.

Method

The DTM/bathymetry model (1883) was extracted based on digitization, and then 3D visualization was performed. The DTM/bathymetry model (2023) was extracted by integrating the latest DTM and field measurements. All multi-source geospatial data must be aligned to the map system using map projection and coordinate transformation (Nixon & Aguado, 2020; Mumuni & Mumuni, 2022). The topographic map has an area of around 2,500 km^2, so it needs to be cropped according to the area of Lake Singkarak boundaries. All of these data are aligned with the projection system and coordinate system. The map projection system used is UTM 47 Southern Hemisphere with the horizontal datum WGS 1984 and the vertical datum earth gravitational model (EGM) 2008. The coordinate system used is 3D Cartesian. Coordinate transformation from the projection system (topographic map of the Dutch East Indies) to the UTM projection system (2017 and 2023 data) using the 3D Projective transformation system with 7 transformation parameters, namely scale, translation (x, y, z), and rotation (ω, φ, κ) (W. Wang, 2002; Trautman, 2006; R. Wang et al., 2021).

After all the data has the same map system, the DTM/bathymetry 1883 and DTM/bathymetry 2023 are extracted. DTM/bathymetry extraction in 1883 was done by digitizing the topographic map of the Dutch East Indies in 1883. Before digitizing, a geometric correction was carried out by equating the map projection system to the Universal Transverse Mercator (UTM) projection system (Datum World Geodetic System (WGS) 1984). This aims to equate the coordinate system so that it is free from blunders so that systematic and random errors are minimized (Ghilani & Wolf, 2006).

The density of the depth contour on the topographic map 1883 is 10 m. In addition, there are also many depth points on the map. The results of the contour digitization and depth points are combined, and then DTM/bathymetry extraction is carried out using 3D interpolation (W. Wang, 2002; Hengl & Evans, 2009; R. Wang et al., 2021). After the DTM/bathymetry model is produced, a pit and spire filter is carried out with bull eye correction. This correction eliminates pits and spires around the main pixel with a tolerance of 1.96σ (Sefercik & Jacobsen, 2006; Gallant et al., 2012).

DTM/bathymetry extraction in 2023 was done by integrating the latest DTM (DTM 2017) and field measurement (depth point sonar 2017 and 2023). Field measurements are divided into two: elevation measurements and bathymetry measurements. Elevation is measured using GNSS-leveling (2017 & 2023) at several sample locations of land topography around the lake, while bathymetry is measured using sonar (2017 & 2023) based on the planned sounding path. Then, the elevation and bathymetry measurement data are combined by tying them to the benchmark (BM) on the edge of Lake Singkarak. All high points used in DTM/bathymetry 2023 are only those that meet the tolerance of 1.96σ.

The DTM/bathymetry 2023 was tested for relative vertical accuracy against field data. Meanwhile, the DTM/bathymetry 1883 was not tested for relative vertical accuracy because it is an official map source with an error close to 0 m (Julzarika et al., 2023). Their error system references all modeling and analysis in this paper against the topographic map (1883) data.

Finally, the analysis of the dynamics of Lake Singkarak was carried out by checking changes in the volume and surface area of the lake by comparing the DTM/bathymetry 2023 with the DTM/bathymetry 1883. In addition, longitudinal profile testing was also carried out following the Semangko fault (west) and the Semangko fault (east) (Krauß, 2018; Julzarika et al., 2021a).

Results and discussion

This study provides spatial information on Lake Singkarak's volume and surface area in 1883 and 2023, as well as the changes over this period. Additionally, it identifies key locations that have experienced significant uplift, subsidence, and landslides between 1883 and 2023.

Volume and surface area of Lake Singkarak 1883-2023

DTM/bathymetry was extracted from the 1883 Dutch East Indies topographic map, and coordinate transformation and map projection were performed using the UTM coordinate system (WGS 1984 datum). Figure 2 (a) shows the DTM/bathymetry 1883, while Figure 2 (b) shows the DTM/bathymetry 2023. Based on the DTM/bathymetry 1883 data, Lake Singkarak has a volume of 18,472,715,824 m^3, an area of 110.21 km^2, and a perimeter of 52.62 km.

DTM Singkarak is obtained by integrating the latest DTM with field data measurements. The latest DTM (2023) is extracted from the results of the DTM 2017 update with vertical deformation 2017-2023. The latest DTM (2023) is similar to DTM/bathymetry (2023). These results are then integrated with the results of field measurements with sonar. The depth results are at a value of 0 to -288 m. From the image, it is clear that Lake Singkarak has cliffs. The lake's shorelines generally exhibit steep slopes, with the eastern side being significantly steeper than the western side. The appearance of the surface to the bottom of the lake shows that the high slope (> 30^o) is along the Semangko Fault (extending from north to south of the lake).

Based on DTM/bathymetry 2023 data, Lake Singkarak has a surface area of 109.07 km^2, a perimeter of 57.129 km, and a volume of 21,110,224,169 m^3. However, the circumference of Lake Singkarak has increased slightly. One cause is the formation of several new capes due to sedimentation and landslides. The morphology of Lake Singkarak has changed, especially on the west and south sides of the lake. The southern area experiences significant sedimentation, driven by soil runoff from rice fields, which is transported at high speeds. The Saniang Baka River also causes high sedimentation, carrying a lot of sediment from upstream. Meanwhile, the western area of the lake often experiences landslides originating from the Bukit Barisan mountains. Rocks and soil from the landslides enter the lake and cause new land to form. In addition, the western area also experiences sedimentation from rivers and rice fields. From 1883 to 2023, the surface area of Lake Singkarak decreased by 1.14 km^2, while the perimeter increased by 4.51 km. Notably, the lake's volume expanded by 2.64 billion m^3.

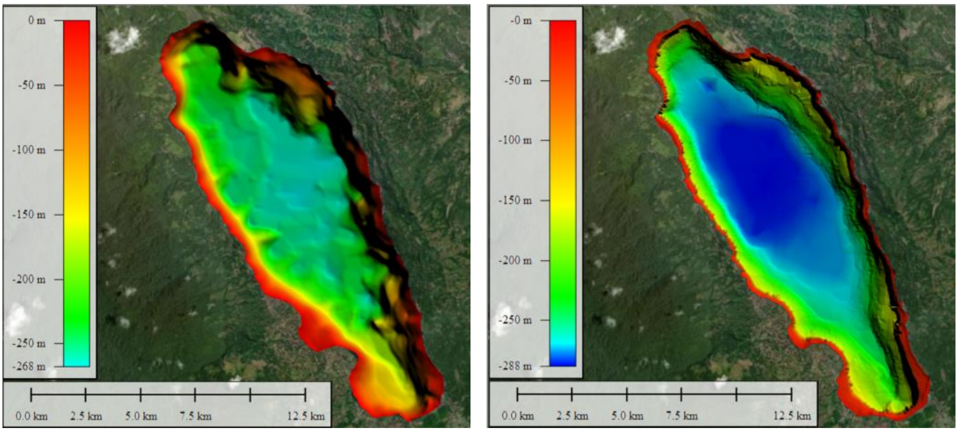

A B

*Fig. 1. The DTM/bathymetry of Lake Singkarak. A. DTM/bathymetry extraction from old topography map 1883 (*Dutch East Indies). B. DTM/bathymetry extraction from the integration of the latest DTM, time-series vertical deformation, and field measurement

Figure 3 illustrates the changes in Lake Singkarak's surface area. The red line marks the lake's boundary in 1883, while the yellow line represents the 2023 boundary.-Several areas have experienced land changes, especially on the south and west sides of Lake Singkarak. From 1883 to 2023, the Singkarak area experienced several major earthquakes, especially in 1926. In that year, according to records from the Dutch East Indies government, a major earthquake caused landslides in and around the lake and caused a large tsunami that destroyed settlements around the lake. One real example of a landslide and tsunami that year can be seen in the changes in the underwater topography of Lake Singkarak. A decrease in the elevation of the bottom of Lake Singkarak marks the basic topographic changes. In addition, it can also be seen in the changes in the hills at the bottom of the lake. In 1883, the hills' texture at the lake's bottom was still clearly visible. However, in the 2023 data, the number and area of the hills at the bottom of the lake had decreased drastically, and the elevation in the middle of the lake had dropped by an average of 20-50 m. As a result of the decrease in elevation, the lake's volume became high. Although the lake's surface area decreased in value, its volume and perimeter increased from 1883-2023.

This condition cannot be seen directly from land but can only be proven by multi-time bathymetry measurements in Lake Singkarak. These observations support the existence of pseudo-dynamics in Lake Singkarak between 1883 and 2023. When viewed from the surface, the volume will appear to decrease due to a decrease in the water level at the edge of the lake. A decrease in the lake's surface area indicates a reduction in the lake's water level. This condition causes people around the lake to think that the volume of the lake has decreased drastically. This is also exacerbated by the statement from the Singkarak hydroelectric power plant, which concluded that there has been a decrease in the lake's surface area, causing its volume to decrease as well. This pseudo-dynamic phenomenon arises from the failure to regularly measure the lake's bottom, leading to the misconception that the lake's elevation remains constant and static. This view overlooks the significant geodynamic and pseudo-dynamic processes occurring in the region.

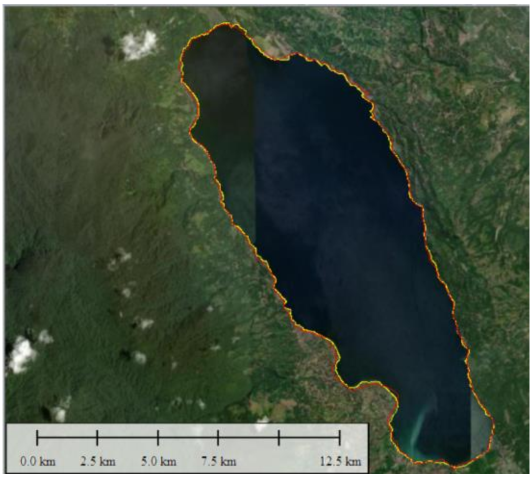

Fig. 2. The surface area changing of Lake Singkarak. The red line is the boundary of Lake Singkarak (1883). The yellow line is the boundary of Lake Singkarak (2023).

Vertical deformation of Lake Singkarak 1883-2023

The vertical deformation of Lake Singkarak from 1883 to 2023 reflects changes in underwater topography caused by various factors such as landslides, earthquakes, excavations, etc. Vertical deformation is obtained from topographic changes in DTM/bathymetry from 1883 to 2023. The vertical deformation values range from 83 to -180 m, with an average annual deformation rate between -15 and -25 cm. Figure 4 (A) shows the result of vertical deformation from 1883 to 2023.

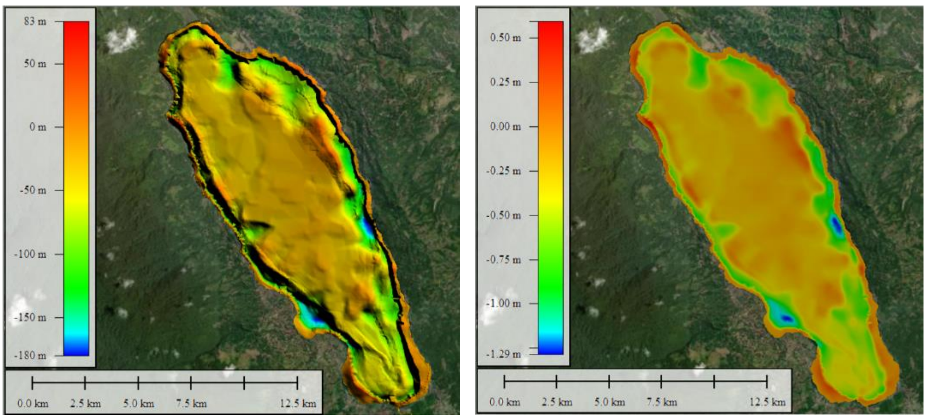

A B

Fig. 3. A. The vertical deformation of Lake Singkarak 1883-2023. B. The average value of vertical deformation in Lake Singkarak 1883-2023

The annual vertical deformation rate of Lake Singkarak from 1883 to 2023 was obtained from the annual average of its vertical deformation data. Based on DTM/bathymetry data (1883-2023) and vertical deformation (2017-2023) in Lake Singkarak, the annual rate of vertical deformation was -1.29 to 0.6 m. The average value of the annual rate of vertical deformation was 10 to -40 cm per year, see Figure 4 (B).

Longitudinal profile of Semangko Fault

A longitudinal profile from south to north was created to assess changes along the Semangko Fault. The Semangko Fault that passes through Lake Singkarak is divided into the East Semangko Fault and the West Semangko Fault. The first check was carried out on the East Semangko Fault. Figure 5 shows a visualization of topographic changes along the East Semangko Fault. The blue line is the lake bed (DTM/bathymetry 1883), while the red line is the lake bed (DTM/bathymetry 2023). From the two lake beds, the difference between the two lake beds (1883-2023) is 5-120 m with an average of 35 m. The area of the lake bed (difference of 40-120 m) is estimated to be a former landslide area due to previous major earthquakes. While the former landslide elevated part of the lake bed, the area remains dominated by subsidence overall. The former landslide along the East Semangko Fault moves westward towards the lake's center. Along the East Semangko Fault, only area Y experiences an increase in the elevation of the lake bed. This area is located directly next to the cliff of the lake bed in the deeper area (blue color) along the line of the East Semangko Fault. Its area has a slope between 30° and 90°.

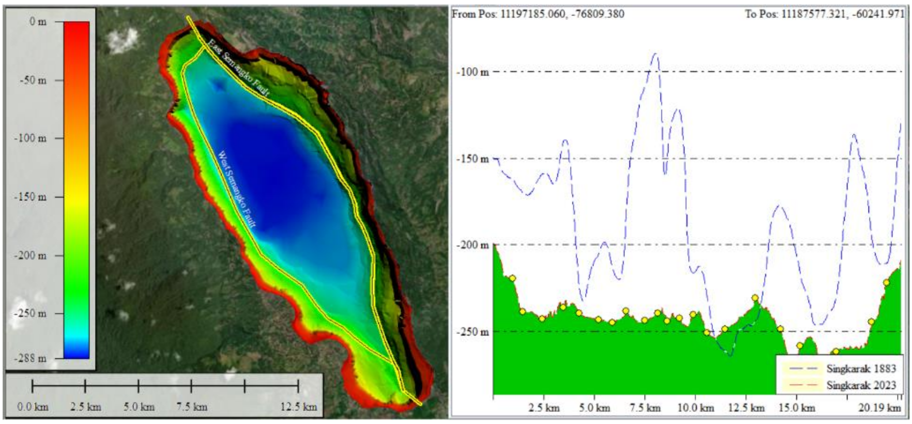

Fig. 4. The longitudinal profile (black line) of the East Semangko Fault (south to north)

Similar conditions also occur in the West Semangko Fault. Based on the transverse profile from south to north, see Figure 6, the lake bed subsidence is more dominant along the West Semangko Fault. The height difference in the lake bed along the West Semangko Fault from 1883 to 2023 ranged from 5 to 130 m, with an average of 30 m. Overall, the West Semangko Fault area predominantly experienced landslides, and its rocks moved eastward (to the middle of the lake). The West Semangko Fault area has a slope of around 25°-70°. The most extreme slope is in the middle of the West Semangko Fault, while the southern and northern areas have gentler slopes (less than 350). The northern area was once a former settlement (ancient kingdom) that sank into the lake, most likely due to a major earthquake. In contrast, the southern area was an agricultural plain that entered the lake and was buried by sedimentation, so this area became softer than the central, northern, western, and eastern areas.

The eastern side of Lake Singkarak, along the East Semangko Fault, is a hilly area with the hardest rocks and lots of hard coral. It is also a dry area with the lowest rainfall. The western side of Lake Singkarak (the western part of the West Semangko Fault) is a mountainous area dominated by forests, fertile soil, and high rainfall. The central area between the West Semangko Fault and the East Semangko Fault is an unstable area affected by large earthquakes and experiences extreme subsidence. It is a place where former rock landslides from both sides of the West and East Semangko Faults gather.

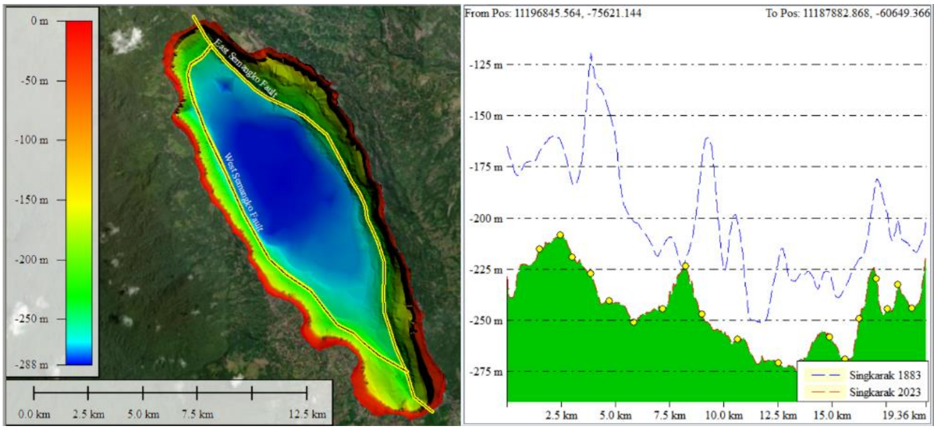

Fig. 5. The longitudinal profile (black line) of the West Semangko Fault (south to north)

Figure 7 (A) shows the potential for reduced volume/landslides (0-100 m) in the period 1883-2023. The orange-red color indicates that the landslide potential is very low, around 0 to -25 m. The cyan-blue color indicates that the landslide potential is very high, around -90 to -100 m. Figure 7 (B) shows the potential for increased landslide volume (0-25 m) in areas prone to landslides due to earthquakes and tectonic subsidence. The area in cyan-blue has a high potential for landslides, while the orange-red area has a low potential.

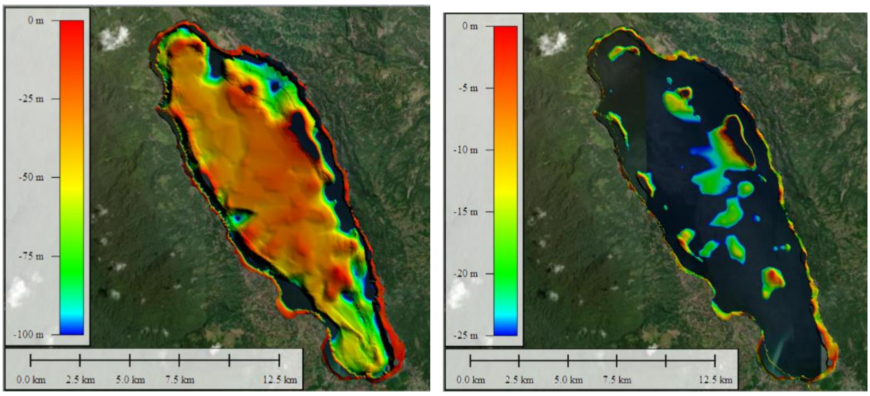

A B

Fig. 6. A. The changing for reduced volume/landslides in the bed floor of Lake Singkarak 1883-2023. B. The high potential of landslide in Lake Singkarak.

Relative accuracy test for DTM/bathymetry 2023

Bathymetry 2023 conducted a vertical accuracy test relative to the field measurements data 2023. The test was conducted using 25 height points (depth). The selection of the 25 points was due to the provision of a minimum number of height test points of 25 for an area of 500 km^2 (ASPRS, 2014). The relative vertical accuracy test of the DTM 2023 yielded an accuracy of approximately 1.5 m. Using 25 height test points, the DTM achieved a vertical accuracy of less than 1 m compared to field measurements.

Discussion

Research on land topography, bathymetry, and vertical deformation in Lake Singkarak has been conducted using field measurements, satellite imagery, and time-series data from Sentinel-1. In addition, other researchers have conducted previous studies related to seismicity records, sediment deposits, rainfall, geomorphology, Semangko fault segmentation, numerical modeling of water quality spatial distribution, and Paleogene syn-rift lacustrine rocks in alluvial fan deltas and modern axial fluvial deltas.

Julzarika & Harintaka, (2019) analyzed the vertical deformation in Lake Singkarak using Sentinel-1 data and field measurements, revealing deformation values ranging from -10 cm to 15.79 cm, indicating tectonic activity along the Semangko Fault. Based on these results, it can be seen that Lake Singkarak is located in an active tectonic (fault) area. The analysis shows that the Singkarak area experienced subsidence in the western region due to landslides, and the eastern region of Singkarak experienced uplift, which was marked by hard rock conditions on the sub-surface. The study's results support the research on the dynamics of Lake Singkarak. The dynamics of vertical deformation state that the active Semangko fault crosses the area and has the potential for earthquakes, landslides on the west side, subsidence, and uplift on the east side.

Julzarika et al. (2021b) conducted a study on the DTM/bathymetry extraction of Lake Singkarak using the LiSAR method. The data used were Sentinel-1 imagery, field bathymetry measurements (sonar), depth data from secondary sources, and geodetic height points around Lake Singkarak. The DTM/bathymetry was extracted in 2017. It was tested for relative vertical accuracy, with a vertical accuracy value of around + 2-3 m. The relative vertical accuracy test compared the results of DTM/bathymetry extraction with field data measurements (sonar). The study's results (DTM/bathymetry 2017 with LiSAR) were used as input data in the DTM/bathymetry 2023 extraction. The DTM/bathymetry 2023 helps determine the dynamics of changes in the volume and surface area of Lake Singkarak.

Wills et al. (2021) examined sediment deposits in Lake Singkarak and concluded that the lake effectively records volcanic and tectonic activity, supporting the dynamic nature of the area and its susceptibility to earthquakes and landslides. The dynamics of the Lake Singkarak area can be known based on the track record of disasters, tectonic movements, seismic dynamics, and volcanic activity. Research by Will et al. (2021) supports that land movement in Lake Singkarak is dynamic, so it has the potential for earthquakes and landslides.

According to Verstappen (1961), Lake Singkarak, based on the Dutch East Indies topographic map of 1883, has a length of 20 km, a width of 7 km, and a maximum water depth of 268 m. Several rivers flow into Lake Singkarak: two large rivers (Sumpur and Sumani Rivers) and several smaller rivers (Verstappen, 1961). The Umbilin River is a natural outlet of Lake Singkarak (Verstappen, 1961; Zen, 1971), and since 1998, a hydroelectric power plant has been built in the western part of the lake and also functions as an artificial outlet for the lake. The central part of the lake has a dome-like structure with a slope angle varying from 0^o to 75^o and is located near the edge of the lake. The results of Verstappen's (1961) research analysis support the results of the DTM/bathymetry (1883) extraction used to determine the dynamics of the volume and surface area of Lake Singkarak. The DTM/bathymetry (1883) is displayed in 3D, making it easier to analyze with geo-visualization. The location of the inlet, outlet, and slope angle of Lake Singkarak can also be determined using the results of the DTM/bathymetry (1883) extraction.

Falah et al. (2023) conducted a study on the segmentation of the Semangko Fault in Lake Singkarak and its surroundings (Sianok segment-Semangko segment) based on active fault mapping using DEM and seismicity. Subduction with oblique dimensions causes the formation of structures in the Sumatra region, especially in Lake Singkarak and its surroundings, through dextral fault movements (Falah et al., 2023). The area also has the potential for earthquakes, and all faults are classified as active. The research results of Falah et al. (2023) support the segmentation of the Semangko Fault in Lake Singkarak with the DTM/bathymetry 1883 and DTM/bathymetry 2023. With the Semangko Fault line, a 3D analysis can be carried out with a longitudinal profile on the Semangko Fault (east and west).

Ajiwibowo et al. (2019) conducted a study on numerical modeling of the spatial distribution of water quality in Lake Singkarak. Field measurement data collected were bathymetry, water level, current velocity, and water quality. The element model uses a surface water model that includes flow, constituent, and sedimentation models. The flow model was validated by matching the current and water elevation between the model and field data. The results of the constituent model show that the Sumpur and Sumani Rivers significantly influence the water quality of the northern and southern parts of Lake Singkarak (Ajiwibowo et al., 2019). Changes in bathymetry at the base of the estuaries of the two rivers are around 30-40 cm per year. The research of Ajiwibowo et al. (2019) helps validate the dynamics of vertical deformation due to sedimentation in the Sumpur and Sumani River estuaries. These dynamics are used in the 2017-2023 bathymetry extraction.

Finaldhi et al. (2016) studied Paleogene syn-rift lacustrine rocks in Lake Singkarak. The study was conducted in the alluvial fan delta and modern axial fluvial delta and aimed to describe the integration of grain texture, fauna analysis, bathymetry, depositional facies, and stratigraphic stack patterns in the modern environment so that the complexity of the potential reservoir geometry and the distribution of quality laterally and vertically are known (Finaldhi, 2018). The research results of Finaldhi et al. (2016) help assist the analysis and validation of the DTM/bathymetry 2023 results, especially in the bedrock and slope sections. In addition, it can also support information related to rocks on the west and east sides of the lake and the modern alluvial and axial fluvial fan delta areas in Lake Singkarak.

Research on the dynamics of lake volume and surface area with multi-source geospatial data is important because it can be used to support regional planning and analysis based on geomorphological and hydrological aspects. The geomorphological aspect is related to morphology and morphometry, such as slope, slope direction, soil vulnerability, morphogenesis, morpho-chronology, and morpho-conservation. The hydrological aspect is related to surface water flow, which includes movement, distribution, and quality of water, as well as water resource management planning. The results of the volume and surface area of the lake can help the government and the community in determining potential landslide locations and safe tourist locations, determining permanent lake boundaries, regulating water resources, and helping to mitigate disasters in this area.

Conclusions

This study concludes that Lake Singkarak's volume and surface area have changed significantly between 1883 and 2023, as determined from DTM/bathymetry data extracted from the 1883 topographic map and the latest field measurements. The change in the volume and surface area of Lake Singkarak was likely caused by the big earthquake and tsunami that occurred in 1926.

Based on the data from the DTM/bathymetry of 1883, Lake Singkarak has a volume of 18,472,715,824 m^3 with an area of 110.21 km^2 and a perimeter of 52.62 km. Based on DTM/bathymetry (2023) data, Lake Singkarak has a surface area of 109.07 km^2 with a perimeter of 57.129 km and a volume of 21,110,224,169 m^3. The surface area of Lake Singkarak (1883-2023) has decreased by 1.14 km^2. In addition, there was an increase in the perimeter of 4.509 km and an increase in the volume of Lake Singkarak by 2,637,508,345 m^3. The annual vertical deformation rate in Lake Singkarak was -1.29 to 0.6 m. The average value of the annual rate of vertical deformation was in the range of 10 to -40 cm per year. The integration of old topographic maps with modern geospatial data provides a valuable geoforensics method, offering precise insights into the long-term changes and geodynamic processes shaping Lake Singkarak.

This research results on the volume and surface area of the lake are important because they can help the government and the community to support regional planning and analysis, as well as other thematic applications based on geomorphological and hydrological aspects. The geomorphological aspect is related to morphology and morphometry, such as slope, slope direction, soil vulnerability, morphogenesis, morpho-chronology, and morphoconservation. The hydrological aspect is related to surface water flow, which includes movement, distribution, and quality of water, as well as water resource management planning.

Acknowledgements: The author wishes to thank the Indonesian National Research and Innovation Agency (BRIN), PT. Citra Bhumi Indonesia (CBI) and The Alaska Satellite Facility (ASF) are responsible for supporting this data research project. The authors are the main contributors to this paper.

Conflicts of Interest: The authors declare no conflict of interest.

Publisher’s Note: Serbian Geographical Society stays neutral with regard to jurisdictional claims in published maps and institutional affiliations.

References

Ajiwibowo, H., Ash-Shiddiq, R. H. B., & Pratama, M. B. (2019). Water quality and sedimentation modeling in Singkarak Lake, Western Sumatra. *International Journal of Geomate, 16*(54), 94–102. https://doi.org/10.21660/2019.54.8145

ASPRS (2014). *Accuracy Standards for Digital Geospatial Data*. The American Society for Photogrammetry and Remote Sensing.

Champion, N., & Boldo, D. (2006). A robust algorithm for estimating digital terrain models from digital surface models in dense urban areas. *Proceedings ISPRS Commission 3 Symposium*, Photogrammetric Computer Vision.

Falah, M. F., Ma, M., Mukti, R., & Helmi, F. (2023). Fault Segmentation of Southern Sumatra (Sianok Segment-Semangko Segment) Based on Active Fault Mapping Through Digital Elevation Model (DEM) and Seismicity. *Journal of Geological Sciences and Applied Geology, 7*(2), 38-51.

Finaldhi, E. (2018). Reservoir Potential of Axial Fluvial Delta vs Alluvial Fan Delta in Syn-Rift Lacustrine: A Modern Study in Lake Singkarak, Sumatra. https://doi.org/10.29118/ipa.0.16.176.g

Finkl, C. W., Benedet, L., & Andrews, J. L. (2005). Interpretation of seabed geomorphology based on spatial analysis of high-density airborne laser bathymetry. *Journal of Coastal Research, 21*(3), 501-514.

Gallant, J. C., Read, a. M., & Dowling, T. I. (2012). Removal of Tree Offsets From Srtm and Other Digital Surface Models. *ISPRS - International Archives of the Photogrammetry, Remote Sensing and Spatial Information Sciences, 34*(B4), 275–280. https://doi.org/10.5194/isprsarchives-XXXIX-B4-275-2012

Geological (2017). Sesar Semangko. Retrieved September 1, 2024, from: http://geologicalmelankolia.blogspot.com/2017/03/sesar-semangko-sumatera.html

Gillani, C., & Wolf, P.R. (2006). *Adjustment Computation: Spatial Data Analysis*. John Wiley & Sons, Inc., Hoboken, New Jersey. The USA.

Hengl, T., & Evans, I. S. (2009). Mathematical and digital models of the land surface. In: T. Hengl & H. I. Reuter (Eds.), *Geomorphometry: Concepts, Software, Applications* (pp. 31–63). Elsevier, Amsterdam.

Julzarika, A. (2021). *The Updated DTM Model using ALOS PALSAR/PALSAR-2 and Sentinel-1 Imageries for Dynamic Topography*. Universitas Gadjah Mada.

Julzarika, A., Aditya, T., Subaryono, & Harintaka. (2020). Comparison of the Latest DTM with DEM Pleiades in Monitoring the Dynamic Peatland. 3rd International Seminar on Research of Information Technology and Intelligent Systems (pp. 604–608). https://doi.org/10.1109/ISRITI51436.2020.9315410

Julzarika, A., Aditya, T., Subaryono, S., & Harintaka, H. (2021a). The latest DTM using InSAR for dynamics detection of Semangko fault-Indonesia. *Geodesy and Cartography, 47*(3), 118–130. https://doi.org/10.3846/gac.2021.12621

Julzarika, A., Aditya, T., Subaryono, S., Harintaka, H., Dewi, R. S., & Subehi, L. (2021b). Integration of the latest digital terrain model (DTM) with Synthetic aperture radar (SAR) bathymetry. *Journal of Degraded and Mining Lands Management, 8*(3), 2759.

Julzarika, A., & Djurdjani, D. (2018). DEM classifications: opportunities and potential of its applications. *J. Degrade. Min. Land Manage, 5*(53). https://doi.org/10.15243/jdmlm

Julzarika, A., & Harintaka. H. (2019). Utilization of Sentinel Satellite for Vertical Deformation Monitoring in Semangko Fault-Indonesia. *ACRS*, 1–7.

Julzarika, A., Laksono, D. P., Subehi, L., Iswandono, E., Dima, A. O. M., Nugraha, M. F. I., & Kayat, K. (2023). The Latest Bathymetry and Topography Extraction of Lake Ledulu from Multi-Source Geospatial Data. *Geographia Technica, 18*(2), 180–195. https://doi.org/10.21163/GT_2023.182.14

Julzarika, A., Rau, M. I., & Yoshikawa, N. (2022). Geospatial mapping using the latest DTM to extract detailed topography and bathymetry. International Society of Paddy and Water Environment Engineering (PAWEES).

Koman, W. A. F., Basith, A., & Julzarika, A. (2023). SAR Bathymetry Review and Its Possibility Implementation in Indonesia. *Journal of Geospatial Information Science and Engineering, 6*(2), 111. https://doi.org/10.22146/jgise.88613

Krauß, T. (2018). A New Simplified DSM-to-DTM Algorithm – dsm-to-dtm-step. https://doi.org/10.20944/preprints201807.0017.v1

Krauß, T., Arefi, H., & Reinartz, P. (2011). Evaluation of selected methods for extracting digital terrain models from satellite born digital surface models in urban areas. *Smpr2011*, 1–7. http://elib-v3.dlr.de/72731/1/krauss2011.pdf

Li, Z., Zhu, Q., & Gold, C. (2004). Digital terrain Modeling: Principles and Methodology. CRC Press. https://doi.org/10.1201/9780203357132

Liu, Y., Zhao, C., Zhang, Q., & Yang, C. (2018). Complex surface deformation monitoring and mechanism inversion over Qingxu-Jiaocheng, China with multi-sensor SAR images. *Journal of Geodynamics, 114*, 41–52. https://doi.org/10.1016/j.jog.2018.01.016

Maune, D. F., & Nayegandhi, A. (2018). *Digital Elevation Model Technologies and Applications: The DEM Users Manual*. American Society for Photogrammetry and Remote Sensing. https://books.google.co.id/books?id=zwiUwwEACAAJ

Mukti, M. M. (2018). Structural Configuration and Depositional History of the Semangko Pull-Apart Basin in the Southeastern Segment of Sumatera Fault Zone. *RISET, 28*(1), 115–128. https://doi.org/10.14203/risetgeotam2018.v28.954

Mumuni, A., & Mumuni, F. (2022). Data augmentation: A comprehensive survey of modern approaches. *Array, 16*, Article 100258. https://doi.org/https://doi.org/10.1016/j.array.2022.100258

NASA (2018). Remote Sensors. NASA. Retrieved September 3, 2024, from: https://earthdata.nasa.gov/user-resources/remote-sensors

Nixon, M. S., & Aguado, A. S. (2020). 10 - Camera geometry fundamentals. In M. S. Nixon & A. S. Aguado (Eds.), *Feature Extraction and Image Processing for Computer Vision* (pp. 483–510). Academic Press. https://doi.org/https://doi.org/10.1016/B978-0-12-814976-8.00010-5

Purnama, Y., Fauzi, A. I., Nurtyawan, R., Sakti, A. D., Nuha, M. U., Anika, N., Putra, R., Siregar, D. I., Prasetyo, B. A., & Julzarika, A. (2023). Long-term water surface monitoring using multi-temporal Landsat satellite data at Singkarak Lake. *AIP Conference Proceedings, 2654*(1).

Sefercik, U., & Jacobsen, K. (2006). *Analysis of SRTM Height Models*. Fifth International Symposium Turkish-German Geodetic Days. http://www.ipi.uni-hannover.de/uploads/tx_tkpublikationen/SRTM_Berlin.pdf

Shen, S. (2018). Simulation study on detecting shallow bathymetry via wavelength. *IOP Conference Series Earth and Environmental Science, 170*(2), 22–55.

Siermann, J., Harvey, C., Morgan, G., & Heege, T. (2014). Satellite derived bathymetry and digital elevation models (DEM). *International Petroleum Technology Conference*. https://doi.org/10.2523/IPTC-17346 –MS

Tarikhi, P. (2012). Liqui-InSAR; SAR interferometry for aquatic body. *International Archives of the Photogrammetry Remote Sensing and Spatial Information Sciences, 34*(B7). https://doi.org/10.5194/isprsarchives-XXXIX-B7-85-2012.

Trautman, A. (2006). Einstein–Cartan Theory. In J.-P. Françoise, G. L. Naber, & T. S. Tsun (Eds.), *Encyclopedia of Mathematical Physics* (pp. 189–195). Academic Press. https://doi.org/https://doi.org/10.1016/B0-12-512666-2/00014-6

Vazirabad, Y. F., & Karslioglu, M. O. (2010). *Airborne Laser Scanning Data for Tree Characteristics Detection*. ISPRS Istanbul Workshop 2010 on Modeling of Optical Airborne and Spaceborne Sensors.

Verstappen, H. T. (1961). Some "volcano-tectonic" depressions of Sumatra, their origin and mode of development. *Proceedings of the Koninklijke Nederlandse Akademie van Wetenschappen, Series B 64*, 428–443.

Wang, R., Zhang, X., & Zhu, B. (2021). A projective transformation-based topology optimization using moving morphable components. *Computer Methods in Applied Mechanics and Engineering, 376*, Article 113646. https://doi.org/https://doi.org/10.1016/j.cma.2020.113646

Wang, T., Belle, I., & Hassler, U. (2015). Modelling of Singapore's topographic transformation based on DEMs. *Geomorphology, 231*. https://doi.org/10.1016/j.geomorph.2014.12.027

Wang, W. (2002). Chapter 31 - Modeling and Processing with Quadric Surfaces. In G. Farin, J. Hoschek, & M.-S. Kim (Eds.), *Handbook of Computer Aided Geometric Design* (pp. 777–795). North-Holland. https://doi.org/https://doi.org/10.1016/B978-044451104-1/50032-0

Wensink, H., & Alpers, W. (2015). *SAR-based bathymetry (Ensycloped)*. Springer. https://doi.org/10.1007/978-0-387-36699-9_207

Wils, K., Daryono, M. R., Praet, N., Santoso, A. B., Dianto, A., Schmidt, S., Vervoort, M., Huang, J. J. S., Kusmanto, E., Suandhi, P., Natawidjaja, D. H., & De Batist, M. (2021). *The sediments of Lake Singkarak and Lake Maninjau in West Sumatra reveal their earthquake, volcanic and rainfall history*. Sedimentary Geology.